On the adsorption/reaction of acetone on pure and sulfate-modified zirconias

On the adsorption/reaction of acetone on pure and sulfate-modified zirconias.

Valentina Crocellà,[a] Giuseppina Cerrato [a,]* and Claudio Morterra[a]

Received (in XXX, XXX) Xth XXXXXXXXX 20XX, Accepted Xth XXXXXXXXX 20XX
DOI: 10.1039/b000000x

In situ FTIR spectroscopy was employed to investigate some aspects of the ambient temperature (actually, IR-beam temperature) adsorption of acetone on various pure and sulfate-doped zirconia specimens. Acetone uptake yields, on all examined systems and to a variable extent, different types of specific molecular adsorption, depending on the kind/population of available surface sites: relatively weak H-bonding interaction(s) with surface hydroxyls, medium-strong coordinative interaction with Lewis acidic sites, and strong H-bonding interaction with Brønsted acidic centres. Moreover acetone, readily and abundantly adsorbed in molecular form, is able to undergo the aldol condensation reaction (yielding, as main reaction product, adsorbed mesityl oxide) only if the adsorbing material possesses some specific surface features. The occurrence/non-occurrence of acetone self-condensation reaction is discussed, and leads to conclusions concerning the sites that catalyze the condensation reaction that do not agree with either of two conflicting interpretations present in the literature of acetone uptake/reaction on, mainly, zeolitic systems. In particular, what turns out to be actually necessary for acetone aldol condensation reaction to occur on the examined zirconia systems is the presence of coordinatively unsaturated O^{2-} surface sites of basicity sufficient to lead to the extraction of a proton from one of the CH_3 groups of adsorbed acetone.

Introduction

The use of acetone (hereafter, Ac) as molecular probe for the surface features of oxidic systems was discouraged long ago by Hair,[1] who considered Ac a non-suitable molecule for the identification/characterization of surface acidic sites. Nonetheless, many authors have since used Ac in the surface study of pure oxides [2-5], mixed oxides [6,7], and zeolitic systems [2,8-12]. The adsorption of Ac on pure silicas and on some silica-based mixed oxides has been recently investigated by means of FTIR spectroscopy and adsorption microcalorimetry[13,14]. The latter study confirmed that Ac is able to establish surface interactions of different kind: (i) it can generate two types of weak H-bonded complexes with scarcely acidic surface OH species (silanols); [13,15] (ii) it forms strong H-bondings with surface hydroxyl groups possessing higher acidity of the Brønsted type, when present; [2,14] (iii) it can coordinate through the lone-pair of the ketonic functionality to coordinatively unsaturated (*cus*) surface cations, acting as Lewis acid centres [2,14]. Moreover, in the presence of proper surface active sites, Ac can undergo the self-condensation reaction termed aldol condensation (hereafter referred to as the a.c. reaction), leading to the dimeric diacetone alcohol species that readily dehydrates to yield mesityl oxide (hereafter, MO).[16]

The study of Ac adsorption on three SiO_2-based oxidic materials of different acidity/basicity [14] led us to the conclusion that necessary condition for the occurrence of the a.c. reaction is the presence of surface *cus* oxide sites (O^{2-}_{cus}) of basic character, whereas the presence of Lewis acid sites may be a necessary but not a sufficient condition for a.c. reaction, and Brønsted protonic centres do not catalise the Ac → MO transformation (at least in non-zeolitic systems). These conclusions were found to contradict the hypothesis presented by Fripiat *et al*. [2,11,12], that implied the presence of Lewis acid sites as the necessary condition for a.c. reaction, as well as the hypothesis of Kubelkova *et al*. [9,17], that ascribed the activation of Ac on zeolitic systems to Brønsted protonic centres.

The present contribution examines the ambient temperature adsorption/desorption of Ac on some pure and sulfate-doped ZrO_2 systems, as well as the relevant reactivity features in the Ac a.c. reaction. During the last two decades, zirconias and, in particular, sulfated zirconias have received much attention, as documented by the incredibly high number of publications which appeared in the literature (see, for instance, ref. 18-28 and references therein). As a consequence, all morphological, surface and reactivity features of these materials are thoroughly known and largely agreed upon. In particular, is well known the presence, at the surface of both pure and sulfate-doped ZrO_2, of Lewis acid centres of medium-high strength (*cus* Zr^{4+} ions) [24,25,27,28] and the existence, at the surface of sulfated ZrO_2 systems, of strong Brønsted acidic sites, [29-31] the strength and reactivity of which is largely due to the presence of nearby Lewis acid sites. [32,33]

The main aim of the present study is to check, by the use of *in situ* FTIR spectroscopy, in which conditions does the a.c. reaction occur on ZrO_2-based systems, trying to verify if, also for these materials, the existence of surface *cus* O^{2-} basic sites is the necessary condition for the Ac self-condensation reaction to MO.[14] A side and somewhat preliminary target of this work is the identification of the type(s) of specific molecular adsorption interaction for Ac and, when formed, MO at the surface of pure and sulfate-doped ZrO_2 systems.

Experimental section

Materials

Pure and sulfated ZrO_2 systems have been synthesized following some long known preparative methods, as briefly reported below:

a) Crystallographically pure *tetragonal zirconia*, referred to in the text as *t*-ZrO_2, was prepared via a sol-gel method and phase-stabilized by the presence of 3 mol% Y_2O_3 in solid solution, as reported in detail elsewhere. [18,27,30] The crystallization in the tetragonal phase was obtained by firing in air at 923 K.

b) *Monoclinic zirconia*, hereafter referred to as *m*-ZrO_2, was obtained by the ambient temperature hydrolysis of Zr isopropoxide, as reported elsewhere. [18,27,30,34] In order to obtain a virtually pure monoclinic crystalline solid, the oven dried ZrO_2 gel was fired in air at 923 K.

c) *Tetragonal sulfated zirconia* samples were prepared by impregnation of crystallographically pure Y-stabilized *t*-ZrO_2 [see point (a)] with a dosed amount of aqueous $(NH_4)_2SO_4$ solution, followed by a thermal treatment of the dried system at 673K. [24,27,30] This step brings about the reactive decomposition of the sulfating agent and guarantees the effective and nominally complete sulfation of the support, while no surface linked sulfate groups are thermally decomposed yet. This system, previously termed "sulfated and non-calcined zirconia", [35] will be referred to in the present text as SZ. A portion of the SZ material underwent a calcination process in air at 923K, bringing about the decomposition of an appreciable fraction of surface sulfates. The latter system, previously termed "sulfated and calcined zirconia", [35] will be hereafter referred to as SZ(C).

In text and figure captions, the symbol of the materials of interest may be followed by a numeral in brackets, indicating the temperature (K) at which the corresponding sample was activated *in vacuo* before adsorption experiments.

BET specific surface area (SSA) (obtained from N_2 adsortpion/desorption isotherms at 77K) and sulfates content (determined by ion chromatography [36]) of all ZrO_2-based materials of interest have been reported elsewhere,[30] and are shown in Table 1.

Reagents

High-purity liquid acetone (Chromasolv for HPLC, 99.8%, Sigma-Aldrich) and mesityl oxide (96%, Sigma-Aldrich), were used without any further purification, and were rendered gas-free by several "freeze-pump-thaw" cycles.

Table 1. Sulfates content and BET SSA of ZrO_2-based samples. [30]

	SSA (m^2/g)	Sulfates loading (SO_4^{2-}/nm^2)
t-ZrO_2	66	-
m-ZrO_2	47	-
SZ	55	8.0
SZ(C)	65	3.1

Techniques

IR Spectroscopy. *In situ* transmission IR spectra were recorded, at 4 cm^{-1} resolution, on a FTIR spectrometer (Bruker IFS 113v, equipped with MCT cryodetector) at "beam temperature" (BT), *i.e.*, the temperature reached by samples in the IR beam. Either in vacuo or under a low adsorptive pressure, BT is estimated to be some 30K higher than room temperature (RT).

Pure ZrO_2 samples were compressed in the form of self-supporting pellets (~15-20 mg cm^{-2}) and mechanically protected with a pure gold frame. Due to the high intensity of sulfate bands, sulfated ZrO_2 systems were inspected in the form of powder thin layers (~10 mg cm^{-2}) deposited from aqueous suspensions on pure Si wafers. All samples were inserted in a homemade quartz IR cell, equipped with KBr windows and characterized by a very small optical path (~2 mm). The cell was attached to a conventional high vacuum glass line capable of a residual pressure $<10^{-4}$ Torr (1 Torr = 133.32 Pa). This setting allowed to perform both samples thermal treatments (usually 2 hr, at the selected activation temperature), and adsorption-desorption cycles of molecular probes in strictly *in situ* conditions.

Before any adsorption experiment, samples were activated *in vacuo* either at BT or at 673 K in order to obtain either a low or a medium-high dehydration stage, respectively.

Ac and MO adsorption/desorption experiments were performed by contacting at BT the activated samples with increasing doses of probe vapour (usually, up to $p \approx 2$-3 Torr), allowing the BT contact for 1 hour, and then evacuating at BT for increasing times (up to 30 min), in order to test the reversibility of adsorbed species. At any step of the adsorption/desorption cycles, *in situ* IR spectra were recorded (128 scans). In all experiments, the equilibrium adsorptive pressure was monitored by a Pirani gauge and a conventional Hg manometer.

Whenever needed, bands resolution of selected ordinate-normalized spectral segments was carried out using the FIT routine by Bruker, that allows the interactive search of the best-fit to the examined experimental absorbance spectral segment on the basis of a number of spectral components imposed by the operator. Unless otherwise specified in the text and/or figure captions, in the present experiments all major spectral parameters (*i.e.*, spectral position, half-band width, percent of gaussian profile) were allowed to float freely, in order to check the reproducibility on passing from one spectrum/experiment to another.

N_2 adsorption at 77K. SSA of all samples was obtained, from N_2 adsorption/desorption isotherms at 77 K, using a Micromeritics ASAP 2020 analyzer. Prior to N_2 physisorption measurements, all samples were outgassed at 523 K for 12 hours to get rid of physisorbed water and other atmospheric contaminants. SSAs were calculated using the standard BET equation method.[37]

Results and discussion

Main surface features of ZrO_2 systems

Surface chemical features, among which surface hydration degree and acidity/basicity, are expected to play an important role in Ac

adsorption processes, as well as in the reaction(s) that Ac may possibly undergo when adsorbed at an oxidic surface. Surface features of both pure and sulfated ZrO_2 systems have been thoroughly investigated long ago in a series of studies [18-36, 38-41] in which IR spectroscopy was mainly adopted.

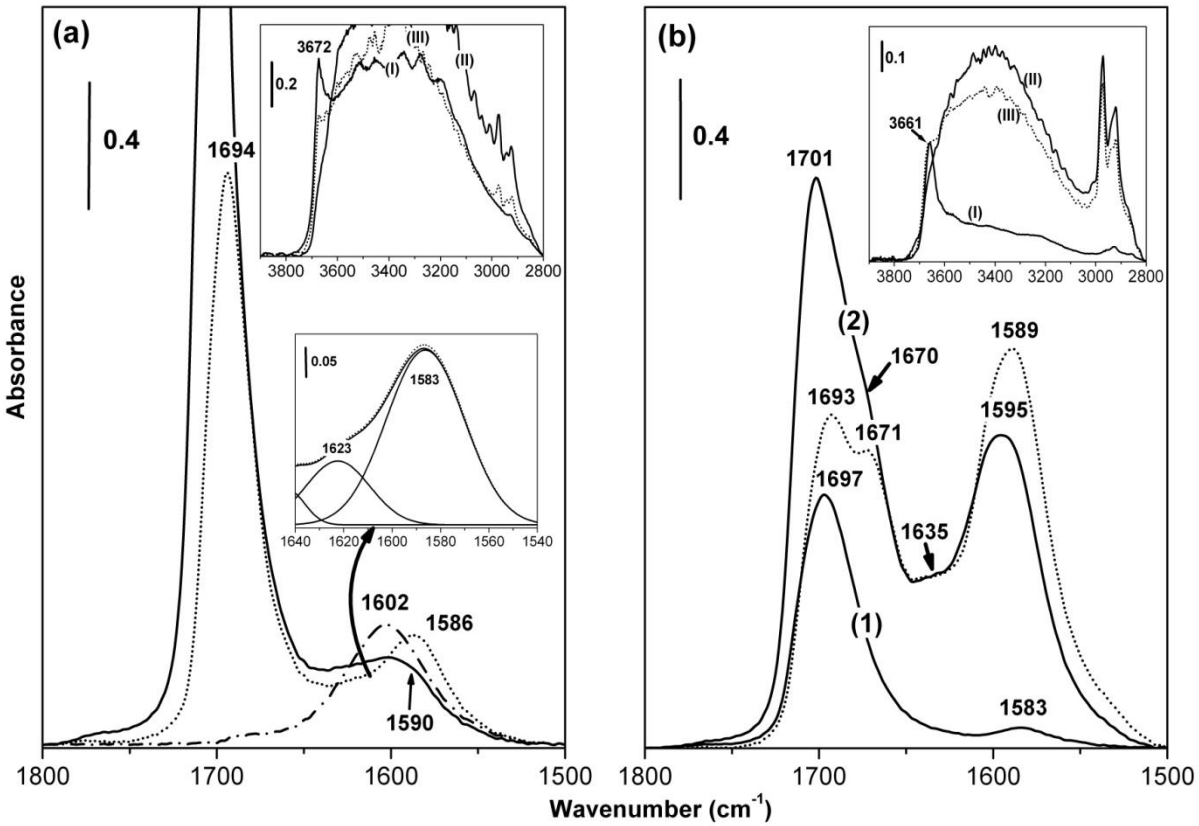

Fig. 1 Differential absorbance spectra (*i.e.*, spectra ratioed against the spectrum of the bare solid, run in the same 1800-1500 cm^{-1} spectral range before gas allowance in the IR cell) relative to the BT adsorption/evacuation of Ac on *t*-ZrO_2. Section (a) - *t*-ZrO_2 activated at BT. These (1800-1500 cm^{-1}) differential spectra were obtained using, as a background, the spectrum of the "water-clean" *t*-ZrO_2 sample activated at 673K, in order to evidence the persistence, after plain BT vacuum activation, of some molecular water (monitored by the δ_{HOH} band at ~1602 cm^{-1}) tightly coordinated at Lewis surface sites. Dot-dashed line: the bare BT sample [*i.e.*, after vacuum activation (2 hr) at BT]. Solid line: after 1 hr contact with 2 Torr Ac. Dotted line: after BT evacuation for 30 min. Section (b) - *t*-ZrO_2 activated at 673 K. No differential spectrum is reported for the bare 673K sample, as it would obviously coincide with the abscissa zero-line. (1): instant contact with 1 Torr Ac; (2) 1 hr contact with 2 Torr Ac; dotted line: after BT evacuation for 30 min. Insets: [section (a), upper panel] absorbance spectra in the 3900-2800 cm^{-1} spectral region of *t*-ZrO_2 after vacuum activation at BT [curve (I)], after 1h contact with Ac [curve (II)], and after 30 min Ac evacuation [curve (III)]; [section (a), lower panel] band-resolved 1640-1540 cm^{-1} segment of the dotted-line spectrum relative to 30 min Ac evacuation. (The full-line spectrum is the reconstructed one, whereas the broken-line trace is the experimental spectrum); [section (b)] absorbance spectra in the 3900-2800 cm^{-1} spectral region of *t*-ZrO_2 after vacuum activation at 673K [curve (I)], after 1h contact with Ac [curve (II)], and after 30 min Ac evacuation [curve (III)].

With specific reference to the ZrO_2 preparations examined in the present work, the main surface features can be summarized as follows:

1) At the surface of plain Y-stabilized *t*-ZrO_2, only one kind of OH species is present (and namely, tri-bridged OH groups; $\nu_{OH} \approx 3660\text{-}3670$ cm^{-1}). [41] By contrast, in the case of plain *m*-ZrO_2, two well resolved OH species, ascribable to terminal (monodentate) and tri-bridged species ($\nu_{OH} \approx 3770\text{-}3780$ and 3660-3670 cm^{-1}, respectively), are usually observed. [1,34a,38,42] Also on Y-stabilized sulfated tetragonal ZrO_2 only (relatively few) tri-bridged OH groups are present, though at a somewhat lower frequency ($\nu_{OH} \approx 3650$ cm^{-1}) as a consequence of the increased surface acidity. [24]
2) On vacuum activated plain ZrO_2 systems, independently of the crystallographic phase, medium-strong Lewis acid sites (*i.e.*, *cus* Zr^{4+} centres) are present. [19, 28]
3) On vacuum activated (non-calcined) SZ, Lewis acid sites are scarse and relatively weak. On the contrary, the vacuum activated (calcined) SZ(C) system possesses an appreciable amount of medium-strength surface Lewis acid sites. [24] In general terms, it can be stated that, on SZ, the abundant degree of surface sulfation drastically reduces the amount of Lewis acidity produced upon surface dehydration, whereas on SZ(C) the sulfation-and-calcination process reduces much less the possible amount of surface Lewis acid sites, and modifies to a very limited extent their acidic strength. [25]
4) In all sulfated systems the presence of surface sulfates induces a Brønsted (protonic) acidity of medium-high strength, that is totally absent on the corresponding pure

oxides. Brønsted acid sites are present at the surface of both non-calcined and calcined sulfated ZrO_2. Still, on SZ(C) the amount of surface Brønsted acid centres is definitely lower, due to the appreciable loss of surface sulfates brought about by the calcination process. [30, 33c]

5) Both pure ZrO_2 phases exhibit good basic properties [43] that can be revealed, for instance, by CO_2 uptake.[20] After the sulfation process, the basicity of *t*-ZrO_2 is virtually extinguished (in general terms, all basic O^{2-}/Zr^{4+} pair sites can be thought to be consumed upon sulfates loading), whereas after the sulfation-and-calcination process basicity is depressed, though not suppressed. In fact, a minor amount of basic O^{2-}/Zr^{4+} pair sites are likely to be recovered during the partial elimination of sulfates brought about by the calcinations step.[35]

Acetone adsorption on pure ZrO_2 systems

(A) The t-ZrO_2 system. Figure 1 reports some spectral patterns relative to Ac adsorption/desorption on t-ZrO_2, vacuum activated at BT [low dehydration stage; section (a)] and 673K [medium-high dehydration stage; section (b)].

The upper inset of figure 1(a) and the inset of figure 1(b) show the spectral patterns in the 3900–2800 cm^{-1} range (the ν_{OH} spectral region) of t-ZrO_2 after the preliminary vacuum treatment [curves (I)], after long Ac contact at BT [curves (II)], and after Ac evacuation at BT [curves (III)]. As expected, the ν_{OH} spectral profile is quite different in the two cases, as a consequence of the different surface dehydration degree achieved. In particular, the signal of OH species free from H-bonding (sharp band centered at ~3660-3670 cm^{-1}, due to tri-bridged OH groups [18, 34a]) is strong and well defined only in the case of the sample activated at 673K, whereas in the case of the BT system the signal of free OH species is scarce, ill-defined and exhibits a huge and broad tailing on the low ν side ($\nu < 3600$ cm^{-1}), due to the ν_{OH} stretching modes of H-bonded OH-containing species (*i.e.*, surface hydroxyls, and some residual molecular water coordinated to surface *cus* Zr^{4+} ions and responsible for the strong δ_{HOH} band at ~1602 cm^{-1} in the background spectrum; *vide infra*). Further to Ac adsorption [curves (II) in the insets], the ν_{OH} spectral region of both samples appears strongly perturbed, in that: (i) all free OH species disappear, and (ii) the broad and unresolved ~3600-3000 cm^{-1} band envelope, strong in section (a) and fairly weak in section (b), exhibits a much increased intensity. These spectral changes indicate that Ac uptake/reaction involves in H-bonding all OH-bearing surface species. After Ac evacuation at BT [curves (III) in the insets], the broad band envelope due to H-bonded OH-bearing species decreases somewhat in both cases, while only a marginal amount of the original free OH band is restored. This means that some adsorbed Ac and, if present, adsorbed reaction products are not reversible and maintain involved in H-bonding interactions most of OH groups.

The main sections (a) and (b) of figure 1 are relative to the range of $\nu_{C=O}$ and $\nu_{C=C}$ vibrational modes and report, in the form of differential spectra, spectral patterns relative to Ac uptake/evacuation. It is evident that, on both samples, the contact with Ac yields adsorbed MO (*i.e.*, the main product of a.c. reaction), in that signals characteristic of adsorbed MO species[2,14] appear in the C=C double bond spectral range (~1550-1600 cm^{-1}). On *t*-ZrO_2(BT) the a.c. reaction occurs only to a very limited extent, whereas on medium-high dehydrated *t*-ZrO_2(673) the formation of MO is far more abundant. This implies that the presence of surface sites that can catalize the a.c. reaction is not an intrinsic property of *t*-ZrO_2, but active sites are produced upon surface dehydration.

Differential spectra of figure 1(a) were obtained using, as a background, the spectrum of *t*-ZrO_2(673) in order to make evident the residual presence on *t*-ZrO_2(BT) of a fair amount of molecular water coordinated to surface cus Zr^{4+} ions acting as Lewis acid sites (see the broad medium-strong band at ~1602 cm^{-1}, due to the "scissors" δ_{HOH} bending vibration [44]). Ac contact with *t*-ZrO_2(BT) produces three main effects: (i) appearance of a very strong and non-resolved $\nu_{C=O}$ stretching band at ~1700 cm^{-1} (solid line spectrum; the band is not shown entirely, due to excessive intensity); (ii) a fair decrease of the δ_{HOH} signal at ~1602 cm^{-1}. The decreased amount of coordinated molecular water indicates that the presence of an excess of Ac and/or a.c. reaction products removes by ligand-displacement some of the water from surface Lewis acid sites; (iii) appearance of a broad and non resolved shoulder band at ~1590 cm^{-1}, ascribed to the early formation of a small amount of (adsorbed) MO (this is the $\nu_{C=C}$ vibrational mode).

When, after long contact, the excess Ac is removed (dotted line trace) the overall spectrum becomes weaker and much better defined. Within the higher-ν $\nu_{C=O}$ band envelop, there is now a vacuum-resistant component apparently centered at ~1695 cm^{-1}, with an evident asymmetry on the low-ν side, while in the $\nu_{C=C}$ spectral region there is now a weak and far better defined band, centered at ~1585 cm^{-1}. The former band envelop is ascribed to the $\nu_{C=O}$ modes of both residual adsorbed Ac and adsorbed MO, whereas the latter signal is ascribable to the $\nu_{C=C}$ vibrational mode of adsorbed MO. Actually, the blown-up band-resolved segment in the lower inset of fig 1(a) shows that, at ~1625 cm^{-1}, (*i.e.*, within the low-ν band envelop) is also present the δ_{HOH} vibration of some residual molecular water, now involved in stronger H-bonding interactions (H-bonding raises the frequency of deformation modes [44]). During BT evacuation, the MO $\nu_{C=C}$ band increases in intensity, as some adsorbed Ac continued to react, and shifts to lower ν, due to a decreased solvent effect exerted by vapour and/or adsorbed Ac.

Differential spectra in figure 1(b) indicate that on *t*-ZrO_2(673) the a.c reaction starts in the very early stages of Ac uptake [after contact with 1 Torr Ac, a tiny $\nu_{C=C}$ stretching band of adsorbed MO appears at ~1583 cm^{-1}; see curve (1)], and then proceeds far more than on the highly hydrated system, as activation at higher T created a higher concentration of sites active for a.c. reaction. After long contact [curve (2)], the strong $\nu_{C=C}$ signal of adsorbed MO moves to ~1595 cm^{-1}, while the corresponding $\nu_{C=O}$ mode becomes an evident shoulder at ~1670 cm^{-1} on the low-ν side of the strong $\nu_{C=O}$ band of adsorbed Ac (~1700 cm^{-1}). The $\nu_{C=C}$ band of adsorbed MO continues to grow during/after the removal of excess Ac (see the dotted-line spectrum), confirming that adsorbed Ac keeps reacting and yields more adsorbed MO, whose $\nu_{C=C}$ band red-shifts to ~1590 cm^{-1} due to a decreased solvent effect caused by Ac evacuation/desorption. Meanwhile, the $\nu_{C=O}$

mode of adsorbed MO has become a stronger and far more evident shoulder (~1670 cm^{-1}) on the low-ν side of the much decreased $\nu_{C=O}$ band of adsorbed Ac (~1693 cm^{-1}).

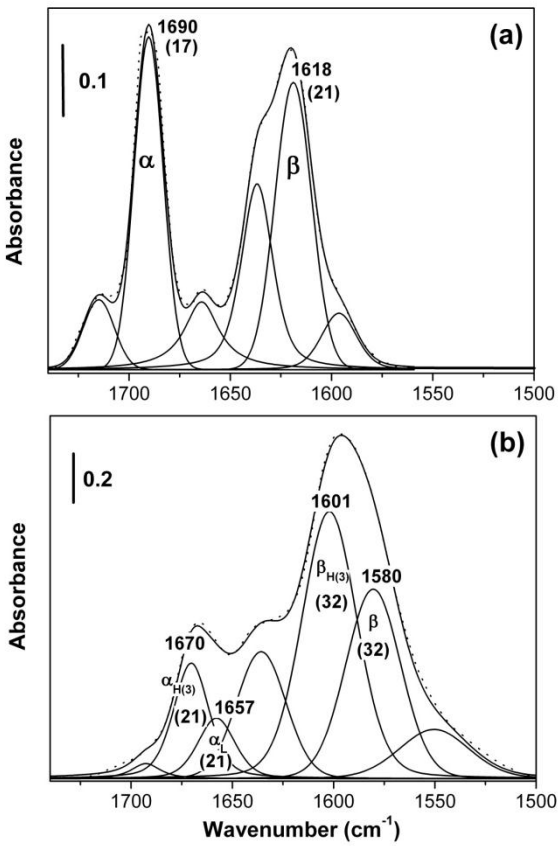

Fig. 2 Reference MO band-resolved spectra in the C=O and C=C double-bond stretching region (1740-1500 cm^{-1}). Section (a): pure MO in diluted CCl_4 solution. Section (b): BT adsorption of (2 Torr) MO on *t*-ZrO_2(673). Full-line complete spectra are the reconstructed ones, whereas broken-line traces are the experimental spectra. Greek letter symbols [α, β, $\alpha_{H(3)}$, etc.] given to some individual spectral components are explained in the text. In section (a), the bands with no letter symbol correspond to satellite (overtone/combination) spectral components of the main $\nu_{C=O}$ (called α) and $\nu_{C=C}$ (called β) vibrational bands; in section (b), the bands with no letter symbol correspond to the non-resolvable envelope of the satellite spectral components of the resolved α ($\nu_{C=O}$) and β ($\nu_{C=C}$) bands. In particular, the strong and broad band centred at ~1635-1640 cm^{-1} corresponds to the non-resolvable envelope of the high-ν satellite band of β bands and the low-ν satellite band of α bands. Two-digit numbers in brackets are the half-band widths (cm^{-1}).

In order to better identify number and nature of the different spectral components present in the complex spectral pattern of figure 1(b), a computer-assisted band resolution has been resorted to. But before describing/assigning the spectral components deriving from Ac adsorption/reaction on *t*-ZrO_2(673), and in order to assist the interpretation of the complex $\nu_{C=O}/\nu_{C=C}$ spectral region, reference computer resolved spectra of MO in CCl_4 solution and adsorbed (at BT) on *t*-ZrO_2(673) were performed. These reference MO spectra are reported in figure 2(a) and (b), respectively.

MO in CCl_4 solution. In the spectral region of interest, it presents two main strong components centered at 1690 cm^{-1} and 1618 cm^{-1}, respectively [figure 2(a)]. The former signal is ascribed to the MO $\nu_{C=O}$ stretching mode (and has been previously termed band α [14]), whereas the latter one is ascribed to the corresponding $\nu_{C=C}$ stretching vibration (previously termed band β [14]). In the absence of specific interactions (as in the present case of MO solution in a non-polar solvent), the α/β integral intensity ratio is very close to 1. Both fundamental double-bond vibrational modes present, on either side, weaker satellite components (overtone/combination modes) that, for MO in CCl_4 solution, are well resolved and centred at 1715/1665 cm^{-1} (satellites of band α), and 1637/1595 cm^{-1} (satellites of band β), respectively.

The reference spectrum 2(a) of MO in CCl_4 solution is the only case here examined in which MO is present in only one form, whereas in all other cases to be considered in the following MO will be present in different forms. For the sake of simplicity, in the following only the various components of the main double-bond α and β stretching modes will be resolved individually, while the envelops of the satellite components will be considered as a whole. This is a necessary simplification that is bound to introduce some uncertainty in the band resolution of complex multiple spectra. In fact, in principle, for each (resolved) α and β component deriving from a specific surface MO interaction, there should be a couple of resolved satellite partner bands, and this is a task virtually impossible to deal with. For this and other reasons, to be mentioned in the following text, it can be stated that: both reproducibility and qualitative meaning of the reported band-resolved spectra are, in general terms, quite good, whereas the quantitative meaning of band intensities and intensity ratios cannot be so good, and their use will be merely indicative of the spectroscopic/reactivity trend.

MO adsorption on t-ZrO_2(673). Figure 2(b) reports, in the $\nu_{C=O}/\nu_{C=C}$ spectral region, the spectrum of MO adsorbed (at BT) on *t*-ZrO_2(673). It is evident that adsorption red-shifted the complex overall MO spectrum, and appreciably modified the overall α/β bands intensity ratio. The best-fit band resolution presented in the figure reveals the splitting of the $\nu_{C=O}$ and $\nu_{C=C}$ fundamental modes in two distinct components, corresponding to MO adsorbed in two different forms. The first species, whose double-bond vibrational modes α and β are red-shifted less, is assigned to the H-bonding interaction of MO with surface tri-bridged OH groups. It presents the $\nu_{C=O}$ vibration [$\alpha_{H(3)}$ in the figure] at ~1670 cm^{-1}, and the $\nu_{C=C}$ one [$\beta_{H(3)}$ in the figure] at ~1600 cm^{-1}. The red-shift of these double-bond bands is, with respect to MO in CCl_4 solution, of some 20 cm^{-1}, corresponding to a medium perturbation strength. (Consider that the weak perturbation of MO in polar $CHCl_3$ solution, in which weak H-bonds can form between solvent and solute, brings about a red-shift of α and β bands of just ~ 6 cm^{-1}). The second MO adspecies is ascribed to the interaction with surface *cus* Zr^{4+} Lewis acid sites, and presents the $\nu_{C=O}$ band (α_L) at 1657 cm^{-1} and the corresponding β_L component at 1580 cm^{-1}. The red-shift of these double-bond bands is, with respect to MO in CCl_4 solution, of some 30-40 cm^{-1}, and corresponds to a rather strong perturbation.

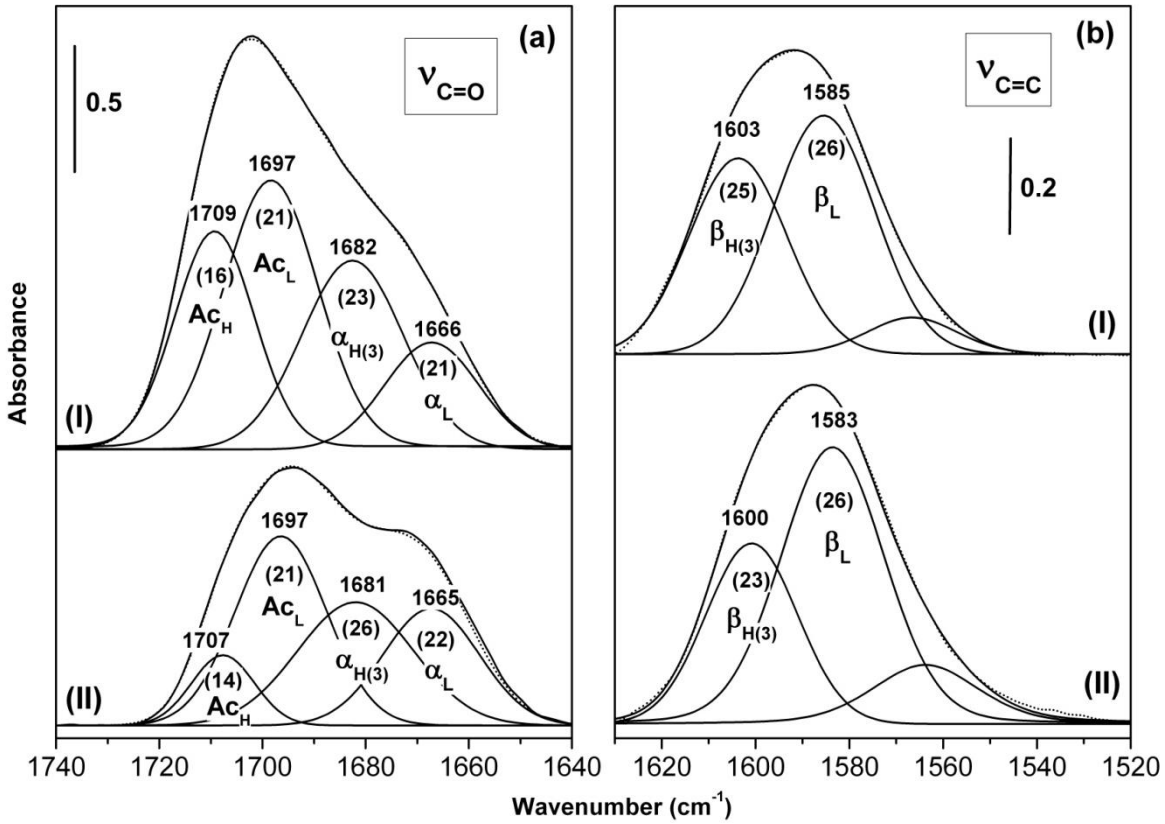

Fig. 3 Band-resolved ordinate-normalized differential spectra relative to BT Ac adsorption/desorption on *t*-ZrO_2(673). Section (a): the $\nu_{C=O}$ spectral region (1740-1640 cm^{-1}); Section (b): the $\nu_{C=C}$ spectral region (1630-1520 cm^{-1}). Full-line complete spectra are the reconstructed ones, whereas broken-line traces are the experimental spectra. Spectral sets (I): 1 hr contact with 2 Torr Ac; Spectral sets (II): After Ac evacuation at BT (30 min). Letter symbols [Ac_H, Ac_L, $\alpha_{H(3)}$, $\beta_{H(3)}$, etc.] given to the individual spectral components are explained in the text. Two-digit numbers in brackets are the half-band widths (cm^{-1}). In section (b), the two bands with no letter symbol, responsible for the evident low-ν asymmetry of the overall bands, correspond to the non-resolvable envelope of the low-ν satellite spectral components of the two resolved ($\nu_{C=C}$) β bands.

Two additional comments on the band-resolved reference spectrum of figure 2(b) are:

(i) Whenever MO uptake leads to interactions of different strength, causing appreciable red-shifts of the two double-bond stretching bands, the lower is the spectral position of the $\nu_{C=C}$ stretching modes (*i.e.*, the stronger is the MO/surface-site interaction), the larger becomes the overall β/α bands integral intensity ratio. For instance, the overall β/α ratio, that is ~1 for MO in CCl_4 solution [figure 2(a)], for MO adsorbed on t-ZrO_2(673) by H-bonding and Lewis coordination has become as large as ~2.5-3. The effect of this prevalent overall intensity of $\nu_{C=C}$ modes over the corresponding $\nu_{C=O}$ modes (due to a larger transition moment and thus extinction coefficient) can be observed also in literature data, [11] and concerns all systems in which the a.c. reaction, leading to the Ac → MO transformation, results in multiple MO adsorption at sites of different strength. Note that the decreased relative intensity of α modes (with respect to the corresponding β modes) caused by medium-strong adsorptive MO interactions renders almost negligible the overall intensity of the high-ν satellite band envelope of α modes (~1690-1700 cm^{-1});

(ii) The double nature of α and β band envelopes of figure 2(b) could not be confirmed by different desorption rates of H-bonded and Lewis coordinated MO because both adspecies are irreversible. But a stepwise MO adsorption experiment, realizing different increasing MO coverages (spectra not shown for brevity), showed that the allowance of the first MO doses first yields a couple of sharp double-bond bands centred at ~1655 and ~1575 cm^{-1}, respectively (*i.e.*, the strongest fraction of Lewis coordinated MO).

Let us now return to the interaction/reaction of Ac on t-ZrO_2(673), shown in figure 1(b) [curve (2) and dotted-line trace]. In both spectra, a flat absorption is evident around ~1635 cm^{-1}. In that spectral position, where the unresolved envelope of the high-ν satellite band of MO β modes and the low-ν satellite band of α modes are expected, also a δ_{HOH} band of coordinated molecular water should be present, as in the a.c. reaction one water molecule is released (for each MO molecule produced) upon dehydration of the diaceton alcohol reaction intermediate. [In fact, a.c. reaction in heterogeneous phase is known to be a self-poisoned process, in that water forms and brings about a surface rehydration that gradually poisons the residual active centres[12]]. The simultaneous presence at ~1635 cm^{-1} of both MO satellite

bands and a water δ_{HOH} signal renders bands identification/simulation very complicate and hardly reliable. It has been thus deemed necessary to carry out band resolution of the spectra of figure 1(b) (as well as of all other similar spectra in the following sections) skipping the 1640-1630 cm^{-1} spectral interval and resolving separately the $\nu_{C=O}$ region (down to 1640 cm^{-1}) and the $\nu_{C=C}$ region (up to 1630 cm^{-1}). The band-resolved spectra of these two regions are reported in figure 3(a) and 3(b), respectively.

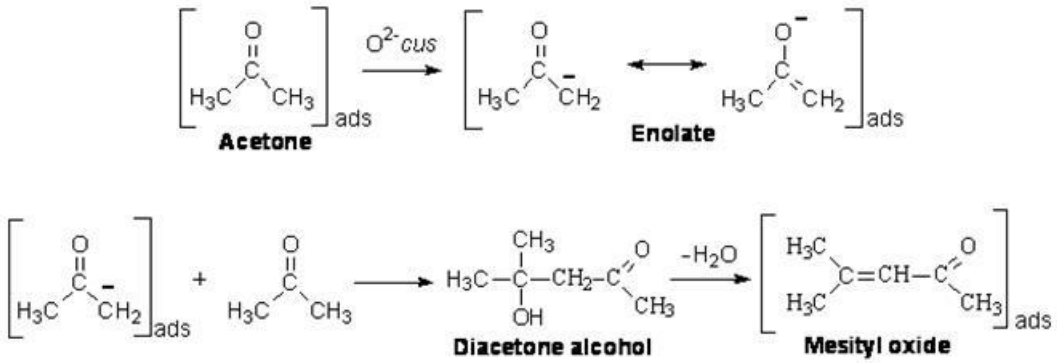

Scheme 1 Aldol condensation of acetone

In spectral set (I) of figure 3(a) [the $\nu_{C=O}$ segment of curve (2) of figure 1(b), relative to a long *t*-ZrO_2(673)/Ac contact] it is possible to single out the following components: (Ac_H) at 1709 cm^{-1}, (Ac_L) at 1697 cm^{-1}, [$\alpha_{H(3)}$] at 1682 cm^{-1}, and (α_L) at 1666 cm^{-1}. The first two bands, generated by two adsorbed forms of non-reacted Ac, are ascribed to Ac interacting by H-bonding with surface (tri-bridged) OH groups and by Lewis acid-base coordination with *cus* Zr^{4+} centres, respectively.[2] Similarly, and on the basis of the discussion of figure 2(b), the lower-ν group of $\nu_{C=O}$ signals is assigned to the adsorption of reaction-formed MO at surface (tri-bridged) OH species and at *cus* Zr^{4+} sites, respectively. The $\nu_{C=O}$ stretching modes of MO species deriving from a.c. reaction are located at ν some 10 cm^{-1} higher than in the case of pure MO adsorbed on *t*-ZrO_2(673). This difference implies a somewhat lower strength of the surface interactions involved and is due to the interfering co-presence of other species (pre-adsorbed Ac and reaction-formed H_2O), that compete for the same sites.

Spectral set (II) of figure 3(a) [the $\nu_{C=O}$ segment of the dotted-line spectrum of figure 1(b)] represents what remains in that spectral range after BT evacuation. Both absolute and relative intensity of all bands changes, owing to the different reversibility of the various adspecies. In particular, both signals relative to adsorbed Ac decrease in intensity, and the reduction of the Ac_H component is far more evident than that of Ac_L (~75% vs. ~30%), due to the weaker interaction with OH groups. As for MO adspecies, only the band $\alpha_{H(3)}$ decreases by some 25%, whereas the band α_L increases by some 20%. The stronger Lewis-coordinated MO adspecies is thus the sole component responsible for the mentioned overall increase of MO formed/adsorbed during the Ac evacuation step.

Spectral sets (I) and (II) of figure 3(b) correspond to the β vibrational modes of the adsorbed MO species just discussed. Band-resolved patterns indicate that, for the $\nu_{C=C}$ vibrational mode, the decreased adsorption strength brought about by the co-presence of (residual) adsorbed Ac and newly-formed H_2O causes an almost null increase of band position with respect to pure MO uptake [Figure 2(b)]. Figure 3(b) also confirms that, during the evacuation step, the H-bonded $\beta_{H(3)}$ species declines slightly, while the Lewis-coordinated β_L component increases somewhat, since non-reacted adsorbed Ac continues to react and more Lewis-coordination sites are made available by Ac_L desorption.

As for the nature of the sites that, on activated *t*-ZrO_2, catalize the a.c. reaction, their identification can be done by comparing the present results with what discussed in a previous work on Ac adsorption.[14] Silica-supported ZrO_2, possessing Lewis acid centres (surface *cus* Zr^{4+} ions) of medium-high strength at all comparable to the acid sites present on pure *t*-ZrO_2, does not yield the a.c. reaction. [14] For this reason, it was concluded that catalytically active centres are not Lewis acid sites but *cus* O^{2-} sites possessing sufficient basicity to extract, by a nucleophilic attack, a proton from one of the CH_3 groups of acetone adsorbed at a nearby surface site. Here, on activated *t*-ZrO_2, this condition is easily met because, on all crystalline zirconias, the simultaneous presence of both basic (*cus* anionic) and Lewis acid (*cus* cationic) sites has been demonstrated long ago.[45] Adsorbed Ac molecules, immobilized as Ac_L species at cus Zr^{4+} sites, or as Ac_H species at surface OH sites, undergo proton extraction from a nearby *cus* O^{2-} site, as shown in Scheme 1.

t-ZrO_2 vacuum activation at increasing temperatures increases much the a.c. reaction activity because thermal surface dehydration decreases the population of OH adsorbing centres and, at the same time, increases the population of Lewis acid (*cus* Zr^{4+}) sites and, to the same extent, the population of catalytically active basic *cus* O^{2-} sites.

(B) The *m*-ZrO_2 system. Figure 4 reports, in the of $\nu_{C=O}/\nu_{C=C}$ spectral range, spectral patterns relative to BT adsorption/evacuation of Ac on *m*-ZrO_2(673). No spectra are reported concerning Ac adsorption on *m*-ZrO_2(BT) as its spectral behaviour, at all similar to that of *t*-ZrO_2(BT), does not yield new information.

The inset of figure 4 shows spectra in the $\nu_{OH}-\nu_{CH}$ spectral region relative to *m*-ZrO_2(673) after the preliminary activation [curve (I)], after Ac contact at BT [curve (II)], and after Ac evacuation at

BT [curve (III)]. As expected on the basis of literature data, [34a, 46] the OH spectral profile of medium-high dehydrated *m*-ZrO_2 is quite different from that of *t*-ZrO_2(673). Two bands of free surface OH species are here present with odd intensity (*ca.* 1 : 2), at ~3775 cm^{-1} (mono-dentate OH, *i.e.*, OH in the coordination sphere of one surface Zr^{4+} ion) and at ~3670 cm^{-1} (tri-bridged OH, *i.e.*, OH in the coordination sphere of three surface Zr^{4+} ions). [18] After Ac adsorption/reaction [curve (II)], both signals of free OH groups disappear, while a broad and unresolved band envelope forms at ~3600-3100 cm^{-1}, indicating that Ac uptake/reaction involves in H-bonding all free OH species. Curve (III) shows that, upon evacuation at BT, the broad band envelope due to H-bonded OH-bearing species decreases somewhat, while a marginal fraction of the band of tri-bridged OH and almost nothing of the band of terminal OH is restored. Also in the case of activated *m*-ZrO_2, some residual adsorbed Ac and/or adsorbed reaction products are not vacuum reversible and maintain the vast majority of surface OH groups involved in H-bonding interactions.

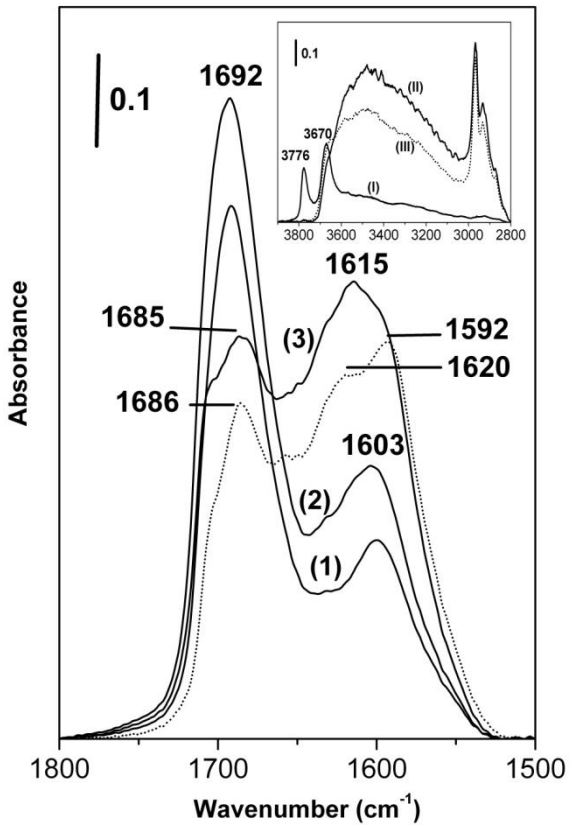

Fig. 4 Differential absorbance spectra (*i.e.*, spectra ratioed against the spectrum of the bare solid, run in the same 1800-1500 cm^{-1} spectral range before gas allowance in the IR cell) relative to the BT adsorption/evacuation of Ac on *m*-ZrO_2(673). (1): instant contact with 1 Torr Ac; (2): instant contact with 2 Torr Ac; (3) 1 hr contact with 2 Torr Ac; dotted line: BT evacuation for 30 min. Inset: absorbance spectra in the 3900-2800 cm^{-1} spectral region of *m*-ZrO_2 after vacuum activation at 673 K [curve (I)], after long contact/reaction with Ac [curve (II)], and after 30 min Ac evacuation [curve (III)].

The differential spectral pattern reported in figure 4 shows that contact with Ac yields the a.c. reaction since the very beginning, as in the earliest stage of Ac uptake [spectrum (1)], a symmetrical band du to the MO $\nu_{C=C}$ mode appears at ~1600 cm^{-1}. With increasing Ac pressure and contact time [see spectrum (2)], the $\nu_{C=C}$ band grows and broadens on the high-ν side, while an unresolved $\nu_{C=O}$ band keeps growing at ~1690 cm^{-1}. After long contact [spectrum (3)], the MO $\nu_{C=C}$ band envelope has become very strong and complex (definitely stronger and broader than in the case of *t*-ZrO_2), while a large high-ν fraction of the complex $\nu_{C=O}$ band has been consumed. This confirms that: (i) a.c. reaction originates from coordinated and/or H-bonded Ac adspecies; (ii) excess Ac and reaction-formed MO compete for the same surface sites, as do water molecules formed in the reaction. (The latters are spectroscopically non evident in the over-crowded 1670-1600 cm^{-1} spectral interval). After prolonged evacuation (see the dotted-line curve), the broad and complex $\nu_{C=C}$ band becomes resolved in two main components (~1620 and ~1590 cm^{-1}), while the $\nu_{C=O}$ band appears much better defined as a consequence of the drastic decrease of the high-ν component due to weaker adsorbed species.

The major difference between Ac adsorption/reaction spectral patterns of *t*-ZrO_2(673) and *m*-ZrO_2(673) [figures 1(b) and 4, respectively] resides in the much broader and ill-defined shape of the $\nu_{C=C}$ band envelope exhibited by the *m*-ZrO_2 system. The difference is most likely related to the existence, on the latter system, of two families of surface OH species instead of one.

MO adsorption on m-ZrO_2. To assist the analysis of the spectral components relative to the complex Ac/*m*-ZrO_2 system, the reference spectrum relative to the BT adsorption of pure MO on *m*-ZrO_2(673), reported in Figure 5, has been examined.

The computer band resolution proposed in the figure, based on the minimal possible number of α and β components, derives from the following assumptions:

(i) There are two α and β components [termed $\alpha_{H(1)}$, $\beta_{H(1)}$, and $\alpha_{H(3)}$, $\beta_{H(3)}$, respectively], relative to the H-bonding interaction with the two families of surface OH species, whereas there is only one α_L and one β_L component, relative to the (unresolved) Lewis coordination to either single or tri-bridged cationic coordinative vacancies. The basis for this hypothesis is threefold: - the adsorption of Lewis bases of different strength at surface Lewis acid sites of (activated) *m*-ZrO_2 never distinguishes different families of sites; [18,19,28c,28d,30] - the acidity of mono- and three-bridged OH of activated *m*-ZrO_2 is quite different [31a], and thus bound to yield H-bonds of different strength; - the comparison between figures 1(b) and 4 highlights the presence, on *m*-ZrO_2, of an additional MO $\nu_{C=C}$ component at ~1620 cm^{-1}, definitely located in the $\nu_{C=C}$ band sub-range typical of H-bonded rather than Lewis-coordinated MO adspecies.

(ii) As in the case of MO on *t*-ZrO_2(673), there will be only one non-resolvable high-ν satellite band of the (resolved) α bands (the band envelope termed I), one unresolved low-ν satellite band of the (resolved) β bands (band envelope II), and one common and unresolved band for both the low-ν satellite band of α bands and the high-ν satellite band of β bands (band envelope III).

(iii) A shoulder at ~1580 cm^{-1} in the β bands domain "imposes" the position/intensity of the strong β_L

component, whereas another pronounced shoulder at ~1648 cm^{-1} "imposes" the position/intensity of the unresolved envelope termed III. The high-ν and low-ν asymmetry of the overall band envelope defines the position/intensity of the unresolved satellite components termed I and II, respectively. Finally, the need for a high β_L/α_L intensity ratio guided the choice of the subsequent best-fit procedure.

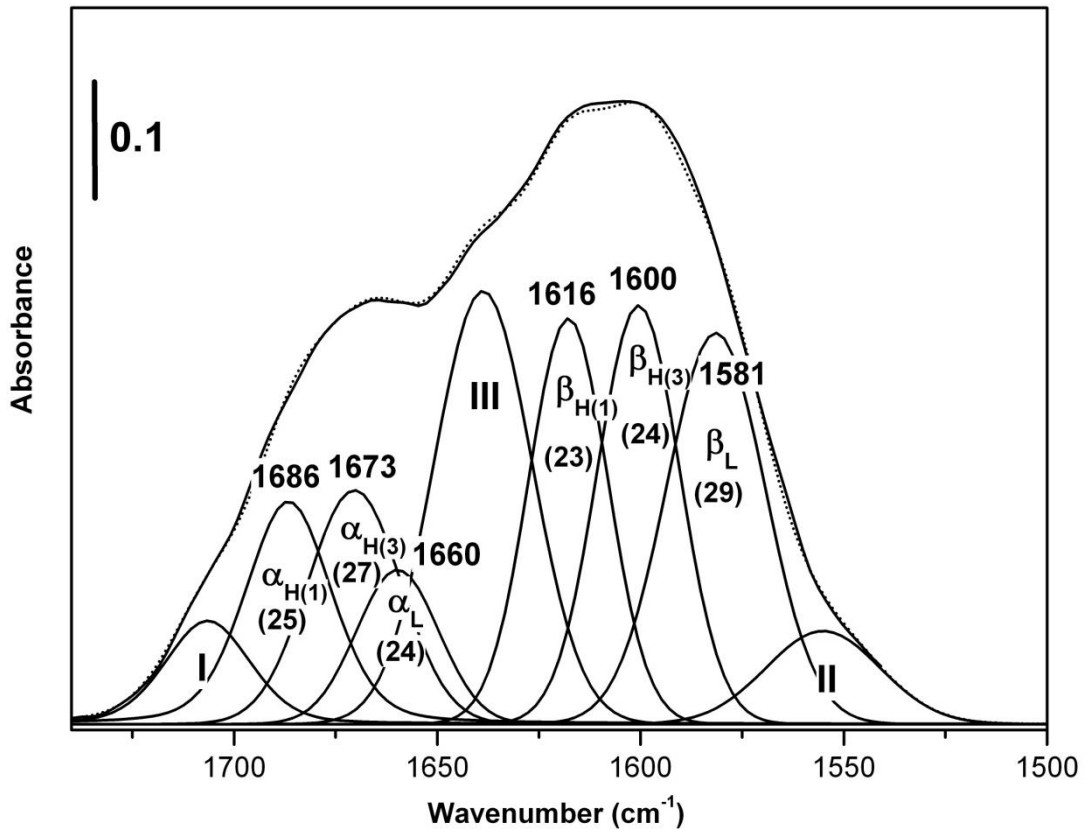

Fig. 5 Band-resolved spectrum in the double-bond stretching region (1740-1500 cm^{-1}) relative to the BT adsorption of (2 Torr) MO on *m*-ZrO_2(673). Full-line complete spectrum is the reconstructed one, whereas the broken-line trace is the experimental spectrum. Greek letter symbols [α, β, $\alpha_{H(3)}$, etc.] given to some individual spectral components are explained in the text; the bands with Roman number symbols correspond to the non-resolvable envelope of the satellite spectral components of the resolved α ($\nu_{C=O}$) and β ($\nu_{C=C}$) bands. In particular, the strong and broad band centred at ~1640-1645 cm^{-1} (III) corresponds to the non-resolvable envelope of the high-ν satellite band of (resolved) β bands and the low-ν satellite band of (resolved) α bands. Two-digit numbers in brackets are the half-band widths (cm^{-1}).

The band-resolution presented in Figure 5 seems quite reasonable. In fact, both α and β modes of the L- and H(3)-components correspond well in position and band-width to those previously obtained [fig. 2(b)] for the simpler *t*-ZrO_2(673) system. Moreover, both α and β modes of the H(1) component correspond well in position and band-width to the average position of α (1682 cm^{-1}) and β bands (1614 cm^{-1}) of MO H-bonded to terminal (mono-dentate) OH groups of silica[2, 13] and silica-based mixed oxide systems.[11, 12, 14]

Returning now to Ac adsorption/desorption on *m*-ZrO_2(673), Figure 6 reports two significant spectra of the spectral pattern of Figure 4 [namely, long contact with Ac (a), and prolonged BT evacuation (b)]. Band resolution was carried out, as explained above for spectra of Figure 3, by simulating separately the ordinate-normalized $\nu_{C=O}$ and $\nu_{C=C}$ spectral regions. The spectral resolution obtained possessed the same good level of accuracy of Figure 3. Only αand β bands are schematically presented in Figure 6 by means of vertical segments indicating bands spectral position and relative intensities. It is evident that all MO spectral species identified in the resolved reference spectrum of pure MO on bare *t*-ZrO_2(673) (Figure 5) are here present, indicating that reaction-formed MO competes (with pre-adsorbed Ac and reaction-formed water) for all types of surface sites. In particular, the $\nu_{C=O}$ spectral region of the upper spectrum (a) indicates:

- (Ac_H) at 1708 cm^{-1} (1709 cm^{-1} on *t*-ZrO_2);
- a non-resolvable band envelope at 1697 cm^{-1} termed [Ac_L + $\alpha_{H(1)}$], due to Ac Lewis coordinated at acid sites (Ac_L) superimposed on MO H-bonded to terminal hydroxyls [$\alpha_{H(1)}$], [Ac_L lies at 1697 cm^{-1} on *t*-ZrO_2, and $\alpha_{H(1)}$ is at 1685-1690 cm^{-1} in the case of pure MO adsorbed on bare *m*-ZrO_2];
- [$\alpha_{H(3)}$] at 1683 cm^{-1} (1682 cm^{-1} on *t*-ZrO_2);
- (α_L) at 1668 cm^{-1} (1666 cm^{-1} on *t*-ZrO_2);
- the corresponding $\nu_{C=C}$ spectral region confirms that the β signal of reaction-formed MO is split in three components centered at 1618 cm^{-1} [$\beta_{H(1)}$; 1616 cm^{-1} for

MO on *m*-ZrO_2], 1606 cm^{-1} [$\beta_{H(3)}$; 1600 cm^{-1} for MO on *m*-ZrO_2] and 1590 cm^{-1} (β_L; ~ 1581 cm^{-1} for MO on *m*-ZrO_2], respectively.

Note that, for MO interacting with surface OH species, the $\beta_{H(3)}$ component is dominant, due to the higher amount of tri-bridged OH species (as monitored by the different intensity of the bands at ~3670 and ~3776 cm^{-1} in the inset of figure 4). Moreover, the (β_L) mode (MO coordinated to surface *cus* Zr^{4+} sites) lies at a frequency some 10 cm^{-1} higher (weaker interaction) with respect to pure coordinated MO, and so turns out to be the vibration of adsorbed MO most affected by the co-presence of other adsorbed species.

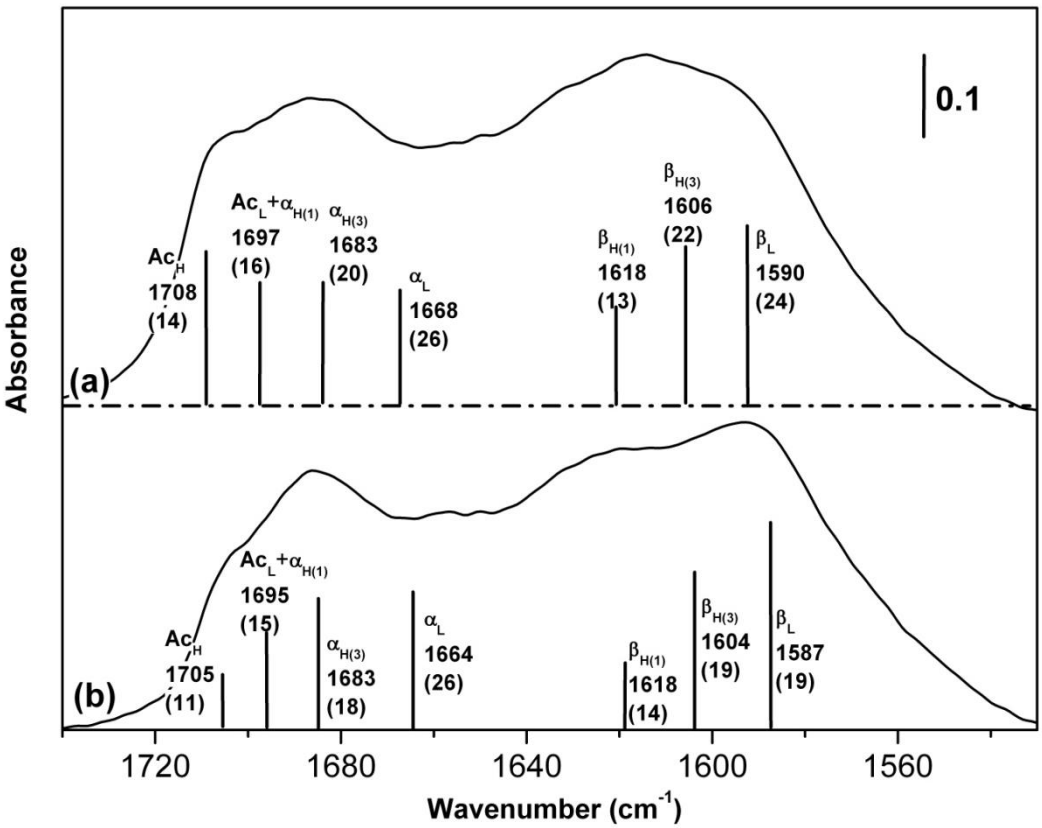

Fig. 6 Schematic presentation of band-resolution obtained, using the two-regions approach already adopted for the spectra of Figure 3, on the ordinate-normalized differential spectra relative to: (a) long time BT Ac adsorption on *m*-ZrO_2(673), and (b) prolonged Ac desorption at BT. Vertical line segments indicate the spectral position of resolved α ($\nu_{C=O}$) and β($\nu_{C=C}$) bands [the position is also indicated by the four-digit numbers (cm^{-1}) on the segments], whereas the length of the segments indicate the relative band intensities. Two-digit numbers in brackets indicate band-widths (cm^{-1}). The letter symbols [Ac_H, Ac_L, $\alpha_{H(3)}$, $\beta_{H(3)}$, etc.] given to the individual spectral components are explained in the text.

Spectrum (b) of figure 6 indicates that, upon evacuation, the components ascribed to the weaker-adsorbed non-reacted Ac species decrease appreciably their intensity, whereas all signals relative to adsorbed MO remain almost unchanged, but for α_L and β_L signals (Lewis coordinated MO adspecies) that increase their integral intensity, as in the case of *t*-ZrO_2. During the evacuation step, some non-reacted Ac continued to react, yielding MO that preferably adsorbs at the strongest available surface sites (*cus* Zr^{4+} ions), while both α_L and β_L components lower their spectral position of few wavenumbers, due to decreased interaction/competition with other adspecies.

Acetone adsorption on sulfated ZrO_2 systems.

Figure 7 reports, in the spectral range of $\nu_{C=O}/\nu_{C=C}$ vibrational modes, the spectral patterns relative to Ac adsorption/evacuation on (activated) sulfated systems SZ [section (a)] and SZ(C) [section (b)], respectively. Since the sulfation procedure does not lead to a thorough elimination of surface hydroxyl species (*i.e.*, the process of surface sulfation is never complete, as amply documented in the literature) [24, 25,31] , the two S-doped samples were vacuum activated at 673 K, in order to attain also for sulphated systems a medium-high surface dehydration stage and so originate a medium level of surface coordinative unsaturation.

The inset of figure 7(a) shows the stretching region of OH groups, after the preliminary vacuum treatment at 673 K, for SZ(673) [curve (I)] and SZ(C)(673) [curve (II)], respectively, whereas trace (III) reports, as a reference, the OH region of plain *t*-ZrO_2 (673). It is quite evident that:

- due to the presence of surface sulfates, the overall surface hydration of sulfated systems is quite low, if compared with that of the plain *t*-ZrO_2(673) system;
- after activation, the residual OH groups are free from interactions of the H-bonding type (no appreciable band tails at $\nu < 3600$ cm^{-1});
- as in the case of plain *t*-ZrO_2(673), only tri-coordinated OH species are present on both SZ systems, though in rather different amounts. In fact, in SZ(C) the thermal elimination of some surface sulfates leads to an

increased OH population;

- surface OH species are represented, for the two S-systems, by bands centered at somewhat different wavenumbers: ~3660 cm^{-1} for SZ(C)(673) (it is almost the "regular" spectral position for tri-bridged OH on *t*-ZrO_2, although the band of SZ(C) is definitely asymmetric on the low-ν side), and ~3640 cm^{-1} with a shoulder at ~3660 cm^{-1} for SZ(673). The main OH peak of SZ(673) is some 20 cm^{-1} lower and, for OH groups of the same coordination type, indicates a definitely higher acidity.

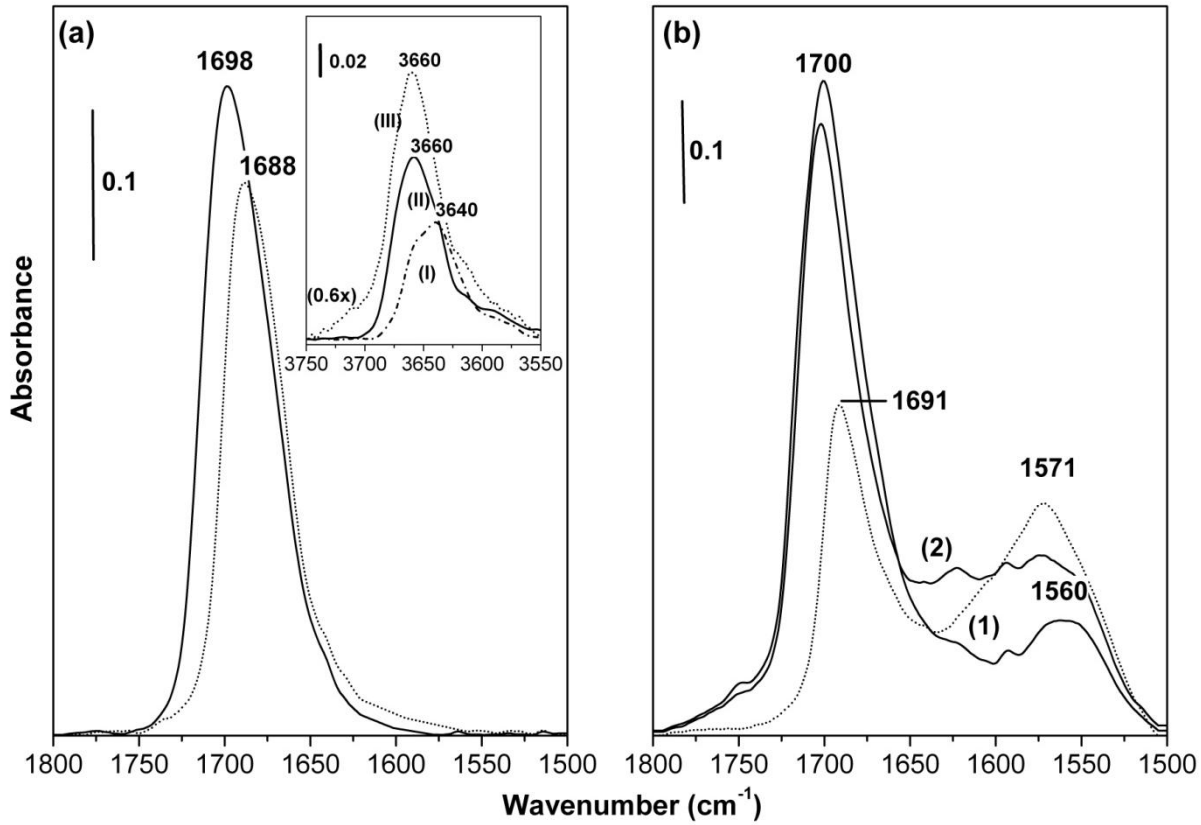

Fig. 7 Differential absorbance spectra (*i.e.*, spectra ratioed against the spectrum of the bare solid, run in the same 1800-1500 cm^{-1} spectral range before gas allowance in the IR cell) relative to the BT adsorption/evacuation of Ac on sulfated ZrO_2 systems. Section (a) – The SZ sample, vacuum activated at 673 K. Solid-line trace: after 1 hr contact with (2 Torr) Ac; dotted-line trace: after BT evacuation for 30 min. Section (b) – The SZ(C) sample, vacuum activated at 673 K. Curve (1): instant contact with 2 Torr Ac; curve (2): after 1 hr contact with (2 Torr) Ac; dotted-line trace: after BT evacuation for 30 min. Inset to section (a): absorbance background spectra in the ν_{OH} spectral region (3750-3550 cm^{-1}) of SZ(673) [curve (I)], SZ(C)(673) [curve (II)] and, as a reference, *t*-ZrO_2(673) [curve (III)]. (The latter OH band was ordinate reduced by a factor 0.6).

(A) The SZ system. Figure 7(a) reports, in the 1800–1500 cm^{-1} range, the spectral pattern relative to Ac adsorption/evacuation on the "sulfated and non-calcined" system SZ(673). (Note that systems like this have been sometimes referred to in the literature as "fully sulfated zirconia" [32], but this definition is clearly not a proper one, due to the mentioned persistence of a non negligible amount of surface OH species [see curve (I) in the inset of figure 7(a)]). It is quite evident that, on SZ(673), no BT a.c. reaction occurs. In fact, the formation of MO could not escape detection since features of (adsorbed) MO would become evident in the $\nu_{C=C}$ spectral range below ~1640 cm^{-1}, as previously observed for MO formed/adsorbed on plain ZrO_2 systems.

A comment/preliminary conclusion seems at this point necessary. The absence of a.c. reaction on the activated sulfated zirconia system carrying the maximum possible amount of surface sulfates and, consequently, the maximum possible concentration of Brønsted acid centres [30, 31a, 31b, 32] indicates that: (i) since surface dehydration at 673 K led to the development of some Lewis acidity (to be confirmed below), the presence of the latter is confirmed not to be a sufficient condition for a.c. reaction to occur. (ii) Unlike what proposed by Kubelkova *et al.* for H- and non-H zeolitic systems, [8,9] on zirconias (and other oxidic systems dealt with elsewhere [14]) the presence of strong protonic acidity of the Brønsted type is not a necessary nor a sufficient condition for a.c. reaction to occur.

In order to test the spectral features of MO on sulfated zirconia and to confirm the absence of reaction-formed MO species on SZ(673), the BT adsorption of pure MO has been carried out also on the two activated S-systems. Section (a) of figure 8 presents, in band-resolved form, the spectrum in the $\nu_{C=O}/\nu_{C=C}$ spectral range relative to BT MO adsorption/evacuation on SZ(673). [In this case, spectra run after evacuation have been resorted to, since with optically very thin thin-layer samples it is easier to distinguish the different (adsorbed) components when the vapour

MO excess and physisorbed MO have been removed].

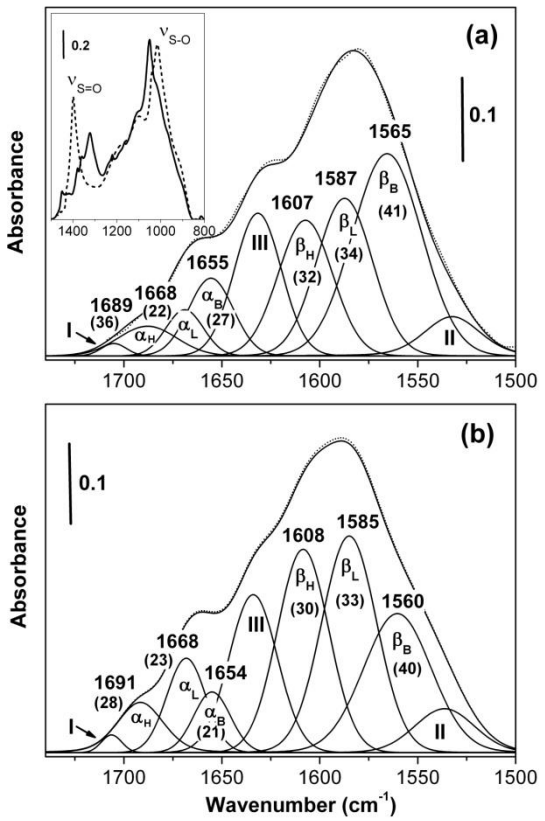

Fig. 8 Computer band-resolved absorbance spectra obtained, in the double-bond stretching region (1740-1500 cm^{-1}), upon MO adsorption on activated S-systems. Section (a): BT adsorption of 2 Torr MO on SZ(673), followed by 30 min BT evacuation. Section (b): BT adsorption of 2 Torr MO on SZ(C)(673), followed by 30 min BT evacuation. Inset: absorbance spectra in the spectral region of sulfates vibrations (1500-800 cm^{-1}) relative to SZ(673), run after vacuum thermal activation (broken-line trace), and after BT contact with 2 Torr MO (solid-line trace). Greek letter symbols (α, β, α_H, etc.) given to some individual spectral components are explained in the text. The bands with Roman number symbols correspond to the non-resolvable envelope of the satellite spectral components of the resolved α ($\nu_{C=O}$) and β ($\nu_{C=C}$) bands. In particular, the strong and broad band (III) centred at ~1635-1640 cm^{-1} corresponds to the non-resolvable envelope of the high-ν satellite band of resolved β bands and the low-ν satellite band of resolved α bands. Two-digit numbers in brackets are the half-band widths (cm^{-1}).

In Figure 8(a) it is possible to observe the splitting of both $\nu_{C=O}$ (the α band) and $\nu_{C=C}$ (the β band) signals in three distinct components, due to the formation of three adsorbed MO species:

1) a first (weak) species is assigned to the H-bonding higher ν interaction of MO with surface tri-bridged OH groups. It presents the $\nu_{C=O}$ vibration (α_H) at ~1690 cm^{-1}, and the $\nu_{C=C}$ stretching mode (β_H) at ~1605 cm^{-1}. Note that $\alpha_{H(3)}$ was at ~1670 cm^{-1} for MO on plain *t*-ZrO_2(673), whereas it lies at the same frequency (~1690 cm^{-1}) in the case of "unperturbed" MO in diluted CCl_4 solution; $\beta_{H(3)}$ was at ~1600 cm^{-1} for MO on plain *t*-ZrO_2(673), and lies at ~1620 cm^{-1} for "unperturbed" MO in diluted CCl_4 solution. These different shifts for α and β spectral components imply that, at least for sulfated zirconia, the main H-bonding interaction of MO with tri-bridged hydroxyls is most probably through the C=C double bond rather than through the carbonyl group. Moreover, the low intensity of α_H and β_H bands is consistent with the weakness of the residual band of non Brønsted acidic OH species [trace (I) in the inset of figure 7(a)], although it is possible that BT evacuation removed a fraction of OH H-bonded MO species;
2) a second adspecies, ascribed to the coordinative interaction of MO with Lewis acid sites (surface *cus* Zr^{4+} ions), presents the α_L band at 1668 cm^{-1} and the corresponding β_L component (much stronger, as expected) at 1587 cm^{-1}. As compared with what reported for plain *t*-ZrO_2 [figure 2(b)], Lewis acidity of the so-called "fully sulfated *t*-ZrO_2" is rather scarce and slightly weaker. In fact, the sulfation process dramatically decreased the residual concentration of surface OH groups and, consequently, thermal dehydration leads to a much decreased surface concentration of Lewis acidic sites.[24] It is interesting to note that MO uptake reveals the surface Lewis acidity of SZ(673), whereas weaker Lewis bases (like, for instance, CO) cannot [26,29]. This means that MO is a base sufficiently strong to ligand-displace surface sulfates from the tri-coordinated configuration assumed after thermal dehydration [30, 32, 34a] to a bi- or mono-coordinated configuration (as in the case of all Lewis bases stronger than the sulfate ion [32]). This ligand-displacement effect on surface sulfates is monitored, in the spectral region of sulfates vibrations (1500-800 cm^{-1}), by the spectral pattern reported in the inset of figure 8(a): the decreased splitting of the $\nu_{S=O}$ and ν_{S-O} modes brought about by MO uptake is similar to that caused, for instance, by the adsorption of acetonitrile [47] or of small doses of water vapour; [29,36]
3) a third pair of $\nu_{C=O}/\nu_{C=C}$ components, centred at 1655 cm^{-1} (band α_B in the figure) and at ν as low as 1565 cm^{-1} (the strong band β_B), is assigned to MO interaction with Brønsted acid sites. This adspecies, characterized by very large double-bond red shifts, represents the strongest MO perturbation and dominates the spectral pattern of figure 8(a). It derives from the abundant presence of surface sulfates that induce, in SZ(673), an abundant Brønsted (protonic) acidity of medium-high strength. [19,30,39,48-50]

Band resolved spectra of Ac adsorption/desorption on SZ(673) are reported in figure 9. The identification of the various spectral components is straightforward and confirms the total absence of MO species. In spectral set (I) of figure 9, corresponding to the $\nu_{C=O}$ segment of the solid-line curve of figure 7(a) (long contact with Ac) the following bands of adsorbed Ac can be singled out: Ac_H at 1710 cm^{-1} (quite weak, as expected); Ac_L at 1698 cm^{-1} (rather strong. It indicates that also Ac is a Lewis base sufficiently strong to ligand-displace tri-coordinated surface sulfates, as confirmed by the sulfate spectral features shown in the figure inset); a band termed Ac_B at ~1680 cm^{-1} (very broad and strong). The first two bands are present with virtually unchanged spectral features (but for the intensity) with respect to

plain *t*-ZrO_2, whereas the last signal, not present on plain *t*-ZrO_2(673), corresponds to the strong H-bonding adsorption of Ac at surface Brønsted (protonic) acid sites. [14]

Spectral set (II) of figure 9 indicates that, after BT evacuation: (i) the low-ν component Ac_H disappears, confirming the labile nature of this H-bonding interaction; (ii) the signal of Lewis-bound Ac_L declines slightly and red-shifts by some 5 cm^{-1}, indicating a somewhat stronger interaction; (iii) Brønsted-bound Ac_B remains almost unchanged ($\Delta\nu_{C=O} \approx$ -4 cm^{-1}), confirming the high strength of this interaction, as suggested by the very low $\nu_{C=O}$ spectral position.

(B) The SZ(C) system. The differential spectral pattern in figure 7(b) shows that the contact of Ac with the "sulfated and calcined" system SZ(C)(673) yields the a.c. reaction, though to a rather limited extent. Bands due to the $\nu_{C=C}$ stretching mode of reaction-formed MO adspecies appear in the low-ν double-bond range of the spectrum immediately after contact with Ac [see curve (1)], continue to grow with contact time [curve (2)], and even after the removal of Ac excess (dotted-line spectrum; also on this system adsorbed Ac keeps reacting, yielding more MO).

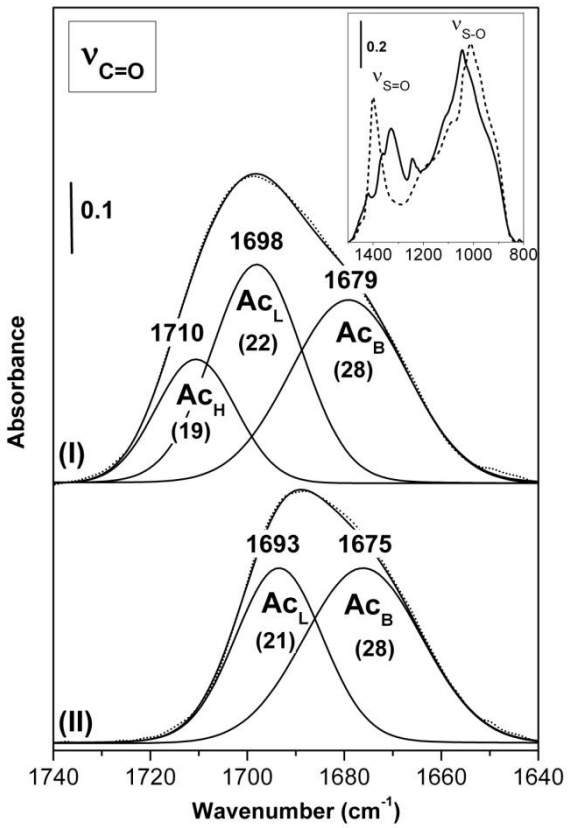

Fig. 9 Two segments in the $\nu_{C=O}$ spectral range (1740-1640 cm^{-1}) of computer band-resolved differential absorbance spectra relative to the Ac/SZ(673) system. Spectral set (I): After long (1 hr) contact with (2 Torr) Ac. Spectral set (II): After BT evacuation for 30 min. Inset: absorbance spectra, in the spectral region of surface sulfates vibrations (1500-800 cm^{-1}), of SZ just after vacuum activation at 673 K (broken-line trace) and after contact with 2 Torr Ac (solid-line trace). The letter symbols (Ac_H, Ac_L, and Ac_B) given to the individual spectral components are explained in the text. Two-digit numbers in brackets are the half-band widths (cm^{-1}).

In order to better identify the spectral components deriving from Ac adsorption/reaction on SZ(C)(673), the preliminary adsorption of pure MO on that system has been carried out. Figure 8(b) presents, in a band-resolved form, the $\nu_{C=O}/\nu_{C=C}$ spectrum relative to the BT adsorption/evacuation of MO on activated SZ(C). As expected, MO on the "sulfated and calcined" system presents the same spectral components of the "sulfated and non-calcined" one [Figure 8(a)], though with different relative intensities. In particular: (i) the signal couples α_H-β_H (MO on surface OH groups) and α_L-β_L (MO coordinated to *cus* Zr^{4+} Lewis acid sites) present virtually unchanged spectral positions and band-widths, whereas the integrated intensities increased appreciably; (ii) the signal couple α_B-β_B (MO interacting with Brønsted acid centers) present lower spectral position (indicating a stronger interaction), and a decreased overall intensity (only MO interacting with the strongest fraction of Brønsted sites is still present). These data are consistent with the interpretation, given long ago,[24] for the role played by the calcination process on crystallographycally stable and "fully sulfated" *t*-ZrO_2 systems: it brings about the selective elimination of the more labile fraction of surface sulfates, located in crystallographically defective positions. The decreased content of surface sulfates leaves, for reaction-formed MO (and any other adspecies), a decreased concentration of protonic (Brønsted) acid sites, as well as an increased surface concentration of "regular" surface OH species which, further to vacuum thermal activation at 673K, yield an increased concentration of Lewis acid sites.

Upon adsorption on activated SZ(C) Ac will find an overall increased concentration of *cus* Zr^{4+} Lewis acid sites. A fraction of the latter sites, located in defective crystal positions wherefrom sulfates have been selectively removed by calcination, is accompanied by an even number of *cus* O^{2-} sites. The spectral pattern of Figure 7(b) indicates that these surface anionic sites possess sufficient basicity to yield the a.c. reaction. Unlike that, in the extended patches of low-index crystal planes ("regular" crystal positions) where most or all sulfate groups remained, the basicity of *cus* O^{2-} sites produced upon vacuum dehydration is hindered by sulfates (as it was for all crystal positions of the "fully sulfated" SZ system). To confirm this hypothesis, Figure 10 presents schematically two band resolved $\nu_{C=O}/\nu_{C=C}$ spectra of the Ac adsorption/desorption pattern shown in Figure 7(b), and namely: 10(a), the spectrum run immediately after Ac contact [spectrum (1) in figure 7(b)], and 10(b) the spectrum run after long contact and evacuation [dotted-line spectrum in figure 7(b)].

As expected, the $\nu_{C=O}$ spectral segment in figure 10(a) is still dominated by the features of adsorbed and non-reacted Ac species, even if the first features of newly-formed MO are already present. The following components can be singled out: Ac_H at 1714 cm^{-1}; Ac_L, still very strong, at 1700 cm^{-1}; α_H (*i.e.*, the weakest form of MO/surface interaction) at 1692 cm^{-1}, competing with Ac_H and still very weak; Ac_B at ~1685 cm^{-1} (note that the $\nu_{C=O}$ band of the strongest-held Ac adspecies lies below that of the weakest-held MO adspecies α_H); α_L at ~1670 cm^{-1}; α_B at 1656 cm^{-1}. The latter two bands are already rather strong, as they belong to the favoured forms of adsorption for newly formed MO. The corresponding $\nu_{C=C}$ spectral segment of figure 10(b), which is free from Ac/MO bands interference, confirms that a major fraction of the first reaction-formed MO yields the strongest-held B-species (strong and broad β_B band at ~1550 cm^{-}

[1]) as well as the strongly-held L-species (strong and broad β_L band at 1570 cm^{-1}), whereas only a minor fraction of reaction-formed MO yields the weakest-held H-species (β_H band at ~1590 cm^{-1}).

The $\nu_{C=O}$ spectral section of figure 10(b), [the dotted-line curve of figure 7(b)] indicates that:

1) variable fractions of the signals ascribable to adsorbed Ac have been eliminated, for effect of both a.c. reaction and evacuation. In particular, virtually all of the weakest-held species Ac_H disappeared (integrated absorbance varied during the reaction from ~5 to ~0.2 cm^{-1}), while the intensity of the stronger-held Ac_L and Ac_B species varied from 8.4 to 3.5 cm^{-1} and from 5.5 to 3.8 cm^{-1}, respectively;
2) the overall $\nu_{C=O}$ spectral range is still not dominated by the α components of the three MO adspecies, because: the extent of a.c. reaction is, overall, rather small, the α_H band at ~1690 cm^{-1} (OH H-bonded MO) is quite weak, due to its partial reversibility to evacuation, and the relative integrated intensity of α_L and α_B bands is intrinsically small. In fact, as anticipated above, the stronger is the adsorption interaction (and, consequently, lower is the $\nu_{C=O}$ stretching band position), the lower is the intensity of the α band, both in absolute terms and with respect to the corresponding β stretching mode. If the corresponding $\nu_{C=C}$ spectral segment of figure 10(b) is considered, it becomes more evident that, after long reaction/evacuation, the dominant MO species is the strongest-held β_B component (~1550 cm^{-1}; its integral intensity varied, from the earliest strage of reaction, from ~2.5 to ~4.0 cm^{-1}), followed by the strong Lewis-held β_L component (1575 cm^{-1}; integral intensity varied from 1.8 to ~3.8 cm^{-1}), while the weakest-held β_H species is present, as expected, in lower amounts (~1595 cm^{-1}; integral intensity varied from 0.7 to ~1.6 cm^{-1}).

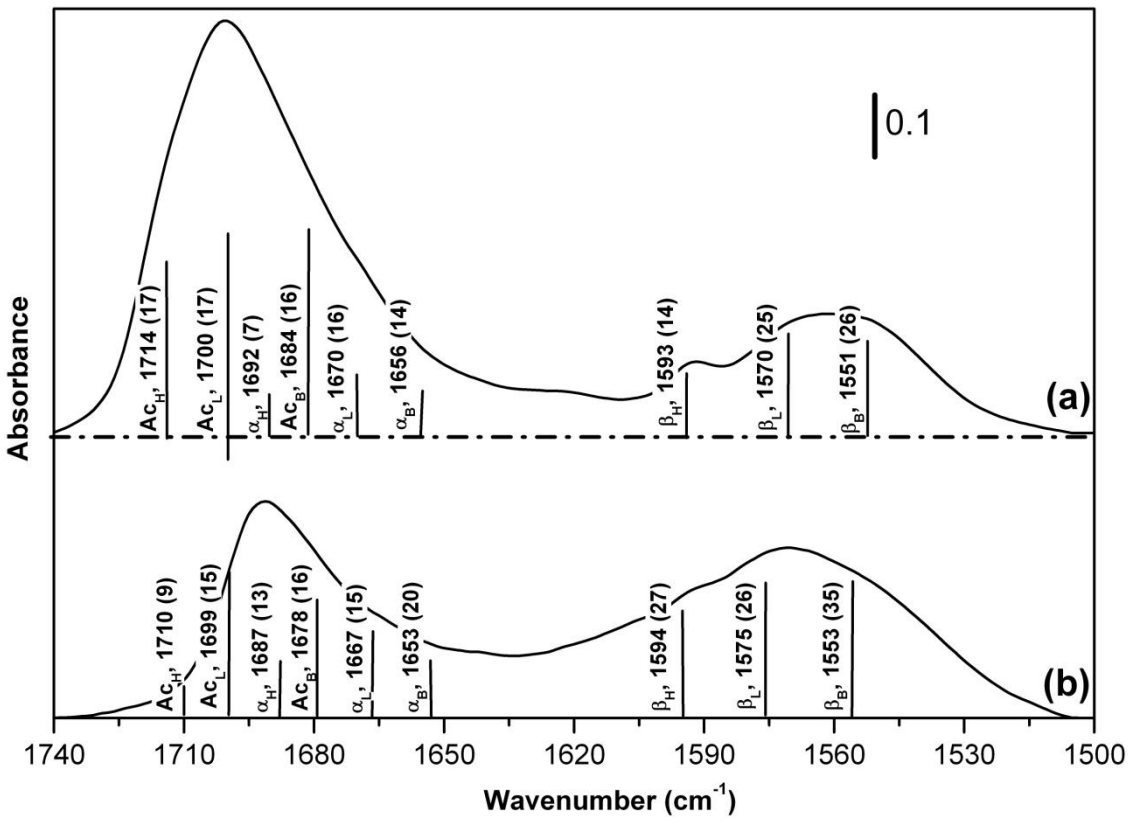

Fig. 10 Schematic presenttion of band-resolution obtained, using the two-regions approach already adopted for the spectra of Fig. 3, on the ordinate-normalized differential spectra relative to BT Ac adsorption/desorption on SZ(C) vacuum activated at 673 K. Section (a): immediate contact with 2 Torr Ac; Section (b): after long (1 hr) contact with 2 Torr Ac and subsequent evacuation at BT for 30 min. Vertical line segments indicate the spectral position of resolved Ac and MO bands [the position is also indicated by the four-digit numbers (cm^{-1}) on the segments], whereas the length of the segments indicate the relative band intensities. Two-digit numbers in brackets indicate band-widths (cm^{-1}). The letter symbols (Ac_H, Ac_L, α_H , β_H, etc.) given to the individual components are explained in the text.

Conclusions

Let us briefly summarize the main achievements of the present contribution, in which the use of *in situ* FTIR spectroscopy allowed to detect and compare the effects of BT adsorption of Ac on pure and sulfate-modified crystalline ZrO_2 systems.

Due to the presence of the carbonyl functionality, Ac acts as a soft base and adsorbs in a molecular form, readily and abundantly, on all types of acid-like sites possibly available at the surface of the examined systems, and namely: (i) surface hydroxyls of any coordination (*i.e.*, for our zirconias, either 1

and 3, or just 3); (ii) *cus* surface Zr^{4+} cations formed upon vacuum thermal dehydration and acting as Lewis acid sites. The latter sites are present to a variable extent on all types of examined zirconias; (iii) proton-releasing surface hydroxyls acting as Brønsted acid sites. These are present only on sulfated zirconias, due to the proton acidic functionality carried by (some of) surface sulfates. The three types of sites lead to interactions of rather different strength that can be evaluated on the basis of the spectral red-shift of the Ac C=O stretching vibration. Computer-assisted spectral band resolution allowed to estimate the ($-\Delta\nu_{CO}$) red-shifts: up to some 10 cm^{-1} in the case of OH H-bonding, ~20 cm^{-1} for Lewis Ac coordination, and up to some 40 cm^{-1} in the case of H-bonding to Brønsted acid sites.

Unfortunately, molar adsorption enthalpies involved in the three types of Ac molecular adsorption could not be determined by adsorption microcalorimetry (unlike what done in several other adsorption studies) because, on all of our zirconias but one (SZ), molecular Ac uptake is followed by the a.c. reaction. The latter leads to the formation of the dimeric diaceton alcohol species (never isolated), that readily dehydrates and leads to MO as the only (IR-observable) reaction product.

MO formation could be monitored spectroscopically by the analytical vibrational modes $\nu_{C=O}$ (located at lower wavenumbers with respect to $\nu_{C=O}$ of Ac adspecies) and $\nu_{C=C}$ (not overlapped with Ac vibrations). Spectral band resolution of reaction-formed MO adspecies turned out to be not so easy due to the presence of satellite (overtone/combination) bands of variable position and relative intensity, located on either side of the two MO analytical modes, and to the symultaneous presence of other adsorbed species (*i.e.*, unreacted Ac and reaction-formed water). Still, with the help of reference spectra of pure MO adsorbed on all systems of interest, a complete set of reasonable/reproducible band-resolved spectra could be obtained and indicated that:

(i) in all cases, reaction-formed MO adsorbs strongly (actually, more strongly than Ac) at all possible families of acid-like surface sites;

(ii) unlike Ac uptake, MO uptake by OH H-bonding (the weakest form of adsorptive interaction) is able to evidence the different acidity of mono-coordinated and three-coordinated hydroxyls at the surface of microcrystalline *m*-ZrO_2;

(iii) the $\nu_{C=C}$ mode of reaction-formed MO, more perturbed by the adsorption process (larger spectral red-shifts) than the $\nu_{C=O}$ mode and not subject to Ac bands overlapping, allowed to evaluate with reasonable accuracy relative amounts and relative stability of the various reaction-formed MO adsorbed species.

As for the controversial identification of surface sites actually responsible for Ac a.c. reaction in an heterogeneous system, the use of several zirconia systems and, in some cases, of different activation conditions allowed us to confirm that determinant for the a.c. reaction to occur is the surface presence of *cus* oxide sites of basicity sufficient to lead to the extraction of a proton from one of the CH_3 groups of Ac adsorbed at a nearby site (*i.e.*, either H-bonded to an OH group or Lewis acid/base coordinated). The present study confirmed that neither of the "acid catalysis" hypotheses present in the literature is valid for the systems examined here. In fact, the surface presence of Lewis acid sites of medium-high strength (indicated by Fripiat *et al* [2,11] as the catalytic sites for a.c. reaction) may possibly be a necessary condition for the reaction to occur, but certainly is not a sufficient condition for either pure or sulfated ZrO_2. Moreover, the surface presence of strong Brønsted acid sites (indicated by Kubelkova *et al.* [9] as the catalytic sites for a.c. reaction in zeolitic systems) in our systems acts *against* the a.c. reaction. In fact, on the non-calcined SZ system (in which all crystal terminations possess abundant Brønsted acidic sulfate groups) the basicity of *cus* oxide sites is suppressed (and no a.c. reaction occurs), whereas on the calcined SZ(C) system, in which some crystal terminations have been liberated from Brønsted acidic sulfate groups, few basic *cus* oxide sites can be present (and the a.c. reaction proceeds, though to a far lower extent than on the corresponding sulfate-free *t*-ZrO_2 system).

Acknowledgements

The present research was funded by Centre of Excellence NIS, whose contribution is gratefully acknowledged, and it was part of the PhD thesis of one of the authors (V. C.).

Notes and references

[a] *Department of Chemistry and Centre of Excellence NIS, University of Torino, via P. Giuria 7, 10125 Torino (Italy).*
E-mail: giuseppina.cerrato@unito.it

1 M. L. Hair, *Infrared Spectroscopy in Surface Chemistry*: M. Dekker: New York, 1967, p. 149.
2 A.Panov, J. J. Fripiat, *Langmuir* 1998, **14**, 3788.
3 B. E.Hanson, L. F.Wieserman, G. W. Wagner, R. A. Kaufman, *Langmuir* 1987, **3**, 549.
4 G.Busca, V.Lorenzelli, *J. Chem. Soc., Faraday Trans. I* 1982, **78**, 2911.
5 M. El-Maazawi, A. N.Finken, A. B.Nair, V. H. Grassian, *J. Catal.* 2000, **191**, 138.
6 W. T. Reichle, *J. Catal*. 1980, **63**, 295.
7 J. A. Lercher, *Zeit. Phys. Chem. N. F.* 1982, **129**, 209.
8 V.Bosacek, L. Kubelkova, *Zeolites* 1990, **10**, 64.
9 L. Kubelkova, J. Ceika, J. Novakova, *Zeolites* 1991, **11**, 48.
10 A. I. Biaglow, J. Sepa, R. J. Gorte, D. White, *J. Catal.* 1995, **151**, 373.
11 A. G. Panov, J. J. Fripiat, *J. Catal.* 1998, **178**, 188.
12 A. G. Panov, J. J.Fripiat, *Catal. Letters* 1999, **57**, 25.
13 V. Crocellà, G. Cerrato, G. Magnacca, C. Morterra, *J. Phys. Chem. C* 2009, **113**, 16517.
14 V.Crocellà, C.Morterra, *J. Phys. Chem. C* 2010, **114**, 18972.
15 (a) D.Griffits, M. K. Marshall, C. H. Rochester, *J. Chem. Soc., Faraday Trans.* 1 1974, **70**, 400; (b) A. G. Okunev, E. A. Paukshtis, Y. I. Aristov, *React. Kinet. Catal.Lett.* 1998, **65**, 161
16 W. T. Reichle, *J. Catal*. 1980, **63**, 295.
17 V. Bosacek, L. Kubelkova, *Zeolites* 1990, **10**, 64.
18 C. Morterra, G. Cerrato, L. Ferroni, L. Montanaro, *Mater. Chem. Phys.* 1994, **37**, 243.
19 C. Morterra, G. Cerrato, V. Bolis, C. Lamberti, L. Ferroni, L. Montanaro, *J. Chem. Soc. Faraday Trans.* 1995, **91(1)**, 113.
20 C. Morterra, G. Cerrato, L. Ferroni, *J. Chem. Soc., Faraday Trans.* 1995, **91(1)**, 125.
21 M. Hino, K. Arata, *J. Chem. Soc. Chem. Commun.* 1980, 851.
22 A. Corma, *Chem. Rev.* 1995, **95**, 559.
23 X. Song, A. Sayari, *Catal. Rev. Sci. Eng.* 1996, **38**, 329.
24 C. Morterra, G. Cerrato, M. Signoretto, *Catal Letters* 1996, **41**, 101.

25 C. Morterra, G. Cerrato, V. Bolis, S. Di Ciero, M. Signoretto, *J. Chem. Soc., Faraday Trans.* 1997, **93(6)**, 1179.

26 S. Melada, M. Signoretto, F. Somma, F. Pinna, G. Cerrato, G. Meligrana, C. Morterra, *Catal Letters* 2004, **94**, 193.

27 C. Morterra, G. Cerrato, S. Di Ciero, *Appl. Surf. Sci.* 1998, **126**, 107.

28 (a) M. I. Zaki and H. Knözinger, Spectrochim. Acta, Part A, 1987, **43**, 1455; (b) H. Knözinger, in Acid-Base Catalysis: Proceedings of the International Symposium on Acid-Base Catalysis, Sapporo, November 28-December 1, 1988, ed. K. Tanabe, H. Hattori, T. Yamaguchi and T. Tanaka, VCH, New York, 1989, p. 147; (c) D. Spielbauer, G. A. H. Mekhemer, M. I. Zaki and H. Knözinger, *Catal. Lett.*, 1996, **40**, 71; (d) W. Stichert, F. Schu¨ th, S. Kuba, H. Knözinger, *J. Catal*., 2001, **198**, 277.

29 C. Morterra, G. Cerrato, F. Pinna, M. Signoretto, *J. Phys. Chem.* 1994, **98**, 12373.

30 C. Morterra, G. Meligrana, G. Cerrato, V. Solinas, E. Rombi, M. F. Sini, *Langmuir* 2003, **19**, 5344.

31 (a) M. Waquif, J. Bachelier, O. Saur, J. C. Lavalley, *J. Mol. Catal.*, 1992, **72**, 127; (b) F. Babou, B. Bigot and P. Sautet, *J. Phys. Chem.*, 1993, **97**, 11501; (c) P. Batamack, G. Coudurier, C. Doremieux-Morin, F. Garin, H. Hachoumi, V. Semmer, J. Sommer and J. C. Vedrine, in Europacat-II, Maastricht, September 3-8, 1995, Symp. No. 5, p. 351; (d) L. M. Kustov, V. B. Kazansky, F. Figueras and D. Tichit, *J. Catal.*, 1994, **150**, 143.

32 C. Morterra, G. Cerrato, F. Pinna, G. Meligrana *Topics in Catal.* 2001, **15**, 53.

33 (a) H. Liu, V. Adeeva, G. D. Lei and W. M. H. Sachtler, *J. Mol. Catal. A*, 1995, **100**, 35; (b) V. Adeeva, J. W. de Haan, J. Jänchen, G. D. Lei, V. Schünemann, L. J. M. van de Ven, W. M. H. Sachtler and R. A. van Santen, *J. Catal*., 1995, **151**, 364; (c) P. Nascimento, C. Akratopoulou, M. Oszagyan, G. Coudurier, C. Travers, J.F. Joly and J.C. Vedrine, in: New Frontiers in Catalysis, eds. L. Guzci, F. Solymosi and P. Tétényi (Elsevier, Amsterdam, 1993) p. 1185; (d) S.X. Song and R.A. Kidd, J. Chem. Soc., *Faraday Trans.*, 1998, **94**, 1333; (e) B.H. Davis, R.A. Keogh, S. Alerasool, D.J. Zalewski, D.E. Day and P.K. Doolin, *J. Catal.*, 1999, **183,** 45.

34 (a) M. Bensitel, O. Saur, J. C. Lavalley, G. Mabilon, *Mater. Chem. Phys.*, 1987, **19**, 249; (b) M. Bensitel, O. Saur, J. C. Lavalley and B.A. Morrow, *Mater. Chem. Phys.*, 1988, **19**, 147; (c) R. A. Comelli, C. R. Vera, J. M. Parera, *J. Catal*., 1995, **151**, 96.

35 V. Bolis, G. Magnacca, C. Morterra, G. Cerrato, *Topics in Catal.* 2002, **19**, 259.

36 C. Sarzanini, G.Sacchero, F. Pinna, M. Signoretto, G. Cerrato, C. Morterra, *J. Mater. Chem.* 1995, **5(2)**, 353.

37 S. J. Gregg, K. S. W. Sing, *Adsorption, Surface Area, and Porosity:* Acad. Press: London, 1982.

38 T. Yamaguchi, Y. Nakano, K. Tanabe, *Bull. Chem. Soc. Jpn.* 1978, **51**, 2482.

39 F. R. Chen, G. Coudurier, J. F. Joly, J. C. Vedrine, *J. Catal.* 1993, **143**, 616.

40 T. Riemer, D. Spielbauer, M. Hunger, G. A. H. Mekhemer, H. Knozinger, *J. Chem. Soc., Chem. Commun.* 1994, 1181.

41 K. T. Jung, A. T. Bell, *J. Mol. Catal. A: Chemical* 2000, **163**, 27.

42 C.R. Vera, C.L. Pieck, K. Shimizu, J.M. Parera, *Appl. Catal. A: General*, 2002, **230**, 137.

43 K. Tanabe, *Mater. Chem. and Phys.*, 1985, **13**, 347-364.

44 (a) N. B. Colthup, L. H. Daly, S. E. Wiberley, *Introduction to Infrared and Raman Spectroscopy*, 2nd ed.; Acad. Press: New York, 1975. (b) K. Nakamoto, *Infrared and Raman Spectra of Inorganic and Coordination Compounds:* J. Wiley & Sons: New York, **1986**.

45 T. Jin, T. Yamaguchi, K. Tanabe, *J. Phys. Chem.* 1986, **90**, 4794.

46 K.T. Jung, A.T. Bell, *J. Mol. Catal. A:* Chemica, 2000, **163**, 27.

47 C. Morterra, G. Cerrato, E. Novarino, P.M. Mentruit, *Langmuir* 2003, **19**, 5708.

48 M. R.Gonzalez, K. B. Fogash, J. M. Kobe, J. A. Dumesic, *Catal. Today* 1997, **33**, 303.

49 F. Haase, J. Sauer, *J. Am. Chem. Soc.* 1998, **120**, 13503.

50 J. F. Haw, J. Zhang, K. Shimizu, T. N. Venkatraman, D. Luigi, W. Song, D. H. Barich, J. B. Nicholas, *J. Am. Chem. Soc.* 2000, **122**, 12561.